Journal of Chromatography A, 1237 (2012) 115–121

Contents lists available at SciVerse ScienceDirect

Journal of Chromatography A

journal homepage: www.elsevier.com/locate/chroma

Low crosslinking imprinted coatings based on liquid crystal for capillary electrochromatography

Ze-Hui Wei, Li-Na Mu, Yan-Ping Huang**, Zhao-Sheng Liu*

Tianjin Key Laboratory on Technologies Enabling Development of Clinical Therapeutics and Diagnostics (Theranostics), School of Pharmacy, Tianjin Medical University, Tianjin 300070, China

ARTICLE INFO

Article history:
Received 19 December 2011
Received in revised form 8 March 2012
Accepted 10 March 2012
Available online 20 March 2012

Keywords:
Capillary electrochromatography
Molecularly imprinted polymer
Liquid crystal
Separation of enantiomers
Coating

ABSTRACT

Low loading capacity is the main problem of molecularly imprinted stationary phase, which is attributed to the high level of crosslinking restricting distortion phenomena of polymer backbone in molecular imprinting. A new approach based on liquid crystal with recognition ability is demonstrated for synthesis of molecularly imprinted polymer coatings in a low level of crosslinking. The resulting low crosslinking (20%) open-tubular imprinted capillary was able to separate enantiomers by means of capillary electrochromatography. The resolution of enantiomer separation achieved on the (*S*)-amlodipine-imprinted capillary was up to 6.36 in less than 2.5 min. The strong recognition ability with a selectivity factor of 1.81 and high column performance of template (up to 23,300 plates/m) were obtained. Performance of imprinting comparable to that recorded in conventional MIP stationary phase was observed. The liquid crystal MIP coatings were also prepared using either (*S*)-naproxen or (*S*)-ofloxacin as template molecule. The resolutions of enantiomers separation were 1.41 and 1.55, respectively. The results illustrate that the synthesis of low crosslinking MIP coatings based on liquid crystal is not only an experimental-simplified process of high performance, but also an approach to produce chiral stationary phase comparable to other chiral stationary phases.

1. Introduction

Molecular imprinting is a popular approach for the preparation of artificial receptors having affinity constants as high as natural ones of the interested molecules [1,2]. The advantages that the highly selective polymers, molecularly imprinted polymers (MIPs), prepared with this technique possess over biopolymers are low cost, and good physical and chemical stabilities. Recently, MIPs have been found in an ever-increasing range of application areas, such as enzyme-like catalysis [3], bio-mimetic sensors [4], solid-phase extraction [5], drug delivery systems [6] and chromatography [7].

Traditionally, MIPs have been prepared by the use of a high level of crosslinker (usually around 80–90%) to construct the memory to the template in the polymer network [1]. In the process of molecular recognition on MIPs, however, the diffusion of a template into and out of imprinted cavity is difficult due to hindered mass transfer produced by the stiffness from high crosslinking network. Therefore, only 15% of the cavities can reuptake a template and the remaining 85% are lost irreversibly [8]. Such low capacity of MIP due to poor site accessibility results in some problems, including lower activity of MIP-based catalyst than theoretical prediction [8] and poor susceptibility to conformational changes in sensor applications [9]. For MIP chromatographic stationary phases, the problem is the peak broadening observed in many cases [7].

To prepare MIPs with affinity not relying on heavy use of cross-linker, an approach for stabilizing binding sites has recently been proposed by Garcinuño et al. [10]. The idea is based on the assumption that an immobilized template will "hold" polymeric chains and complementary functionalities together, preventing the collapsing of the binding sites. In the presence of immobilized template, low cross-linked bulk imprinted polymers have showed positive effect on molecular recognition [10,11]. In spite of comparable affinity to high crosslinked MIP, the crosslinked MIP in the presence of the immobilized template showed very low binding capacity.

Another strategy to achieve more accessible sites is to prepare liquid-crystalline MIP, as shown by Mauzac et al. [12–19]. In their studies, by virtue of the orientation imposed on the mesogenic side-groups and the coupling between the mesogenic side-groups and the polymer backbone, low levels of cross-linking (5–20 mol% of the monomer units) were sufficient to imprint the memory of a template. Because chemical crosslinking is placed by physical crosslinking, the resultant MIPs have similar selectivity but

* Corresponding author. Fax: +86 22 23536746.
** Corresponding author.
E-mail addresses: huangyp100@163.com (Y.-P. Huang), zhaoshengliu@sohu.com (Z.-S. Liu).

0021-9673/$ – see front matter © 2012 Elsevier B.V. All rights reserved.
doi:10.1016/j.chroma.2012.03.041

much higher capacity compared with classical MIPs since the non-covalent reversible interactions between mesogenic moieties can confer a stiffness on the polymer network. As a result, the mass transfer of template can be improved due to the decrease of crosslinker level. Recently, catalysts [18] and sensors [19] based on liquid-crystalline MIPs have been reported. However, no liquid-crystalline MIPs were used as stationary phase due to the nature of elastomer of such MIP, which is hard to resist the high pressure from HPLC.

Capillary electrochromatography (CEC) is a microcolumn separation method designed to combine the advantage of the high separation efficiency of capillary electrophoresis (CE) and high selectivity offered by HPLC [20]. Up to now, three formats can be used for MIP-based CEC, namely particle-packed column [21–27], monolithic columns [28–33] and capillary coatings [34–42]. However, peak tailing of template was observed still and the problem is a long-standing challenge.

In view of the facts above, if a general way of solving this problem is found and established, it would open new perspectives to the field of enantiomer separation. The objective of this work was to take advantage of liquid-crystalline for design of MIP stationary phase. An imprinted stationary phase based on liquid crystal was prepared with a format of MIP coating inside a capillary at a low level of crosslinker and evaluated by CEC. With electroosmotic flow (EOF) as flow driver instead of hydraulic flow, the distortion of MIP film is avoided. Three chiral template imprinted capillary coatings were prepared under the low crosslinking density in the presence of liquid crystalline monomers. The characterization of EOF and the ability of enantiomer separation for the new MIP-coated capillary were investigated.

2. Experimental

2.1. Chemicals

Liquid crystalline monomer, 4-methyl phenyl dicyclohexyl propylene was purchased from Hebei Meixin (Hebei, China). 3-(Trimethoxysilyl) propyl methacrylate (γ-MPS) was from Acros (Geel, Belgium). Methacrylic acid (MAA) was obtained from Beijing Donghuan Chemical Reagent (Beijing, China). Ethylene glycol dimethacrylate (EDMA) was from Sigma (St. Louis, MO, USA). 2,2′-Azobis (2-isobutyronitrile) (AIBN) was supplied by Special Chemical Reagent Factory of Nankai University (Tianjin, China). *S*- and *rac*-amlodipine (AML) were from Hengshuo Sci & Tech Corp. (Hubei, China). *S*-Naproxen (NAP) and *rac*-naproxen were obtained from Zhejiang Xianju Pharmaceutical Co. Ltd. (Zhejiang, China). *S*- and *rac*-ofloxacin (OFX) were from Sigma–Aldrich (St. Louis, MO, USA). Acetonitrile (ACN, HPLC grade) was purchased from Fisher (New Jersey, USA). Other analytical reagents were from Tianjin Chemical Reagent Co. Ltd. (Tianjin, China). Fused-silica capillaries with 100 μm ID and 375 μm OD were purchased from Xinnuo Optic Fiber Plant (Hebei, China).

2.2. Preparation of liquid crystal MIP capillary

A fused-silica capillary was flushed with 1 M NaOH solution followed by water for at least 30 min each. Then the capillary was filled with a solution of 4 μL of γ-MPS in 1 mL of 6 mM acetic acid, and the solution was kept in the capillary for 1.5 h. The capillary was then flushed with water and dried with a flow of nitrogen. A pre-polymerization mixture containing imprinted molecules (0.08 mmol), liquid crystalline monomer (0.96 mmol or 1.04 mmol for *S*-OFX), MAA (0.32 mmol), EDMA (0.32 mmol or 0.24 mmol for *S*-OFX) and AIBN (1.8 mg) were dissolved in 0.635 mL toluene–isooctane (7/3, v/v) or toluene/ACN (7/3, v/v) for *S*-OFX. The pre-polymerization mixture was sonicated for 10 min then introduced to the capillary using a syringe. The capillary was sealed at both ends with a rubber septum and incubated in a water bath (53 °C) for polymerization. After polymerization, to remove any unreacted reagents, the capillary was immediately flushed using a hand-held syringe with acetonitrile and methanol/acetic acid (9:1, v/v), respectively. A detection window was created at a distance of 11.5 cm from the outlet end of the MIP-coated capillary by burning out 2–3 mm segment of the polyimide outer coating. A blank capillary column without imprinted molecule was prepared in the same way.

2.3. Capillary electrochromatography

Electrochromatographic experiments were carried out on a K1050 system (Kaiao, Beijing, China) equipped with a UV detector. A Lenovo personal computer with CXTH-3000 software for capillary electrophoresis was used. The total length of the capillary was 41.5 cm and effective length (MIP-based stationary phase) was 30.0 cm. The electrolyte was a mixture of acetonitrile and different ratios of buffer with different pH values. All the buffers were made using doubly distilled water and filtered with 0.2 μm membrane.

The resolution (R_s) was calculated according to the equation $R_s = (t_2 - t_1)/0.5(W_2 + W_1)$ and the number of theoretical plates (N) was calculated by the equation $N = 16(t_R/W)^2$, where t_R is the retention time and W is the width at the baseline between tangents drawn to inflection points for the peak.

The degree of enantiomer separation was represented by a normalized separation index $\Delta t_R/t_{R1}$, where Δt_R is the difference in the elution times of the enantiomers at peak maximum and t_{R1} is the retention time of the first eluted enantiomer.

2.4. SEM characterization of the MIP coatings

Scanning electron microscopy (SEM) was used for the characterization of MIP-coated capillaries. The fused-silica capillary samples were cut to 2–3 mm in length, and cemented into aluminum SEM planchets. Samples were sputter-coated with gold before obtaining images. All scanning electron micrographic images were obtained using a Shimadzu SS-550 scanning electron microscope, operated at 15 kV and a filament current of 60 mA.

3. Results and discussion

3.1. Preparation of liquid crystal MIP coatings

To form a successful polymer coating, the most important parameter of polymerization is porogen. The density and structure of the final polymer coating are highly dependent on the nature of the porogen [34]. Successful systems of porogen to prepare MIP-coated capillary for CEC consist of toluene [34], ACN [35], and a mixture of solvents, e.g., ACN/2-propanol [36], toluene/ACN [37] and a ternary mixture of toluene/isooctane/DMSO [40]. In our study, experiments showed that the liquid-crystal monomer could be dissolved in toluene well, and a mixture of toluene/isooctane was found to be a good porogen to prepare MIP coating in a capillary. However, (*S*)-ofloxacine could not be dissolved in the mixture of toluene/isooctane, so toluene/ACN was used as the porogen to prepare (*S*)-ofloxacine-imprinted coatings capillary.

Polymerization time and temperature are the key factors to control the porous properties, e.g., thickness and porosity. In this study, it was found that higher temperature (60 °C) resulted in occluded columns. Lower reaction temperature is thought to provide enhanced imprinting [1]; however, longer reaction times had

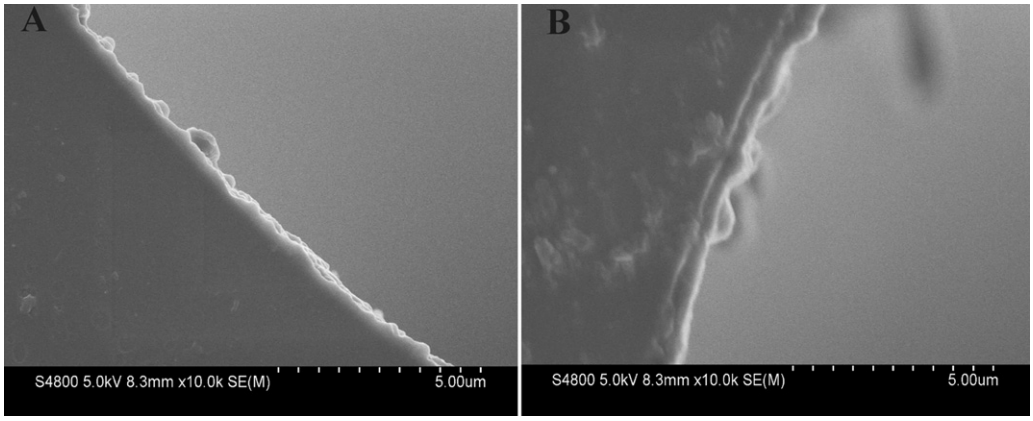

Fig. 1. Scanning electron micrograph of liquid crystal (A) and conventional (B) MIP-coated capillary using (*S*)-amlodipine as template molecule.

to be used to prepare MIP coatings in capillary. Furthermore, no significant improvement in resolution was observed when columns made at lower temperatures (48 °C) were compared to those produced at higher temperatures. As a result, 53 °C was found to be the optimized temperature for polymerization.

In addition, it was found that the low crosslinking MIP coatings required a strict reaction time. Too short polymerization time, e.g., 1.5 h, was not ideal, because the MIP coating was too thin. As a result, the electeochromatograms for the separation of enantiomers were all similar to those of non-imprinted capillaries. When the reaction time was prolonged to 2 h, MIP monolith formed was completely occluded. It was found that the optimum reaction time was 1.75 h.

The feasibility of the synthesis of MIP with lower amounts of cross-linker in the presence of liquid crystal was studied at a fixed ratio of MAA (functional monomer; 20%, molar ratios). In general, the increase in the content of cross-linking agent causes an increase in selectivity of resulting MIP and imprinting does not work when the concentration of cross-linker approaches 12% [1]. In our study, even if the level of crosslinker was as low as 5%, the (*S*)-AML-MIP coating capillary could still provide baseline separation of *rac*-AML in spite of decreased selectivity than the liquid crystal MIP with higher level of crosslinker (Table 1). In this case, it can be seen that even if the selectivity factor was not very high, separation of enantiomers can be achieved.

Visualization of the microstructure of the resulting MIP films was accomplished through scanning electron microscopic investigations on several capillary segments. Fig. 1A shows a SEM cross-sectional view of liquid crystal MIP-coated capillaries with AML imprinting. A layer of MIP with a thickness around 0.1–0.2 μm covering the inner surface of the capillary was obtained. As a comparison, the SEM of liquid crystal-free MIP-coated capillaries with AML imprinting was provided, which shows a layer of MIP with a thickness around 0.2–0.3 μm (Fig. 1B).

Table 1
Effect of the different levels of liquid crystalline on (*S*)-amlodipine imprinted coatings column.

Liquid crystal ratio	N_R (m^{-1})	N_S (m^{-1})	α	$\Delta t/t_R$	R_s
60%	23,300	22,200	1.81	0.81	6.36
65%	15,000	20,600	1.72	0.72	5.33
70%	2540	20,000	1.18	0.18	1.64
75%	1650	18,600	1.16	0.16	1.24

CEC conditions: separation voltage, 3–25 kV; temperature, 25 °C; UV–vis detector, 238 nm; ACN/10 mM acetate (pH 3.6) (80/20, v/v).

3.2. Capillary electrochromatographic enantiomer separation

Imprinting effect of low crosslinking MIP coating with liquid crystalline monomers was evaluated by enantiomer separation in CEC mode. Fig. 2A and B illustrates the separation of *rac*-AML on the (*S*)-AML-imprinted coated capillaries, depicting the characteristic elution order and the selective retention of the template. In the optimum conditions, the resolution of two enantiomers was 6.36. Compared with previously reported MIP coating with a thickness of 0.1–0.2 μm [34], pronounced improvement in column efficiency and resolution was observed. The strong recognition ability with a selectivity factor of 1.81 and high column performance of the template (up to 23,300 plates/m) were obtained. In contrast, a nonimprinted reference capillary prepared with liquid crystalline monomers showed no enantiomeric separation ability (Fig. 2C). Longer elution time of template on blank column than imprinted column was observed because the EOF of blank column (11.0 cm/min) is smaller than imprinted column (12.9 cm/min), which may be due to the different polymerization kinetics of MIP prepared in the presence or absence of, as well as different templates.

To assess the superiority of the low crosslinking MIP coatings over those prepared with the normal level of crosslinking, the liquid crystalline-free MIP coating with 80% (molar ratios) EDMA, a

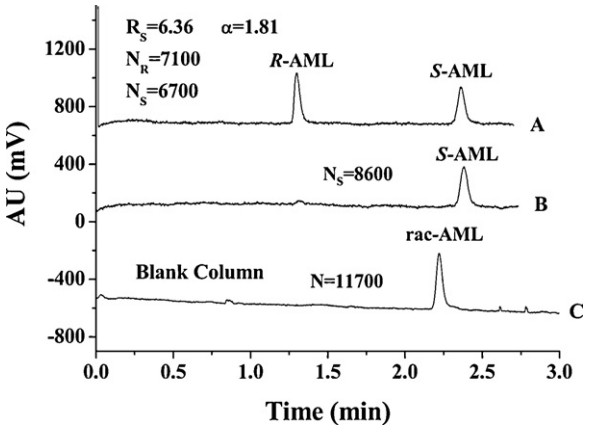

Fig. 2. Electrochromatograms of *rac*-AML (A), *S*-AML (B) on *S*-AML imprinted capillary and *rac*-AML on non-imprinted capillary (C) demonstrating the imprinting effect and identifying the peaks. Elution order: (*R*)-amlodipine followed by (*S*)-amlodipine. Conditions: capillary, 100-μm inner diameter, 41.5-cm total length, and 30.0-cm effective length; separation voltage, 25 kV; temperature, 25 °C; UV–vis detector, 238 nm; acetonitrile/10 mM acetate (pH 3.6) (80/20, v/v).

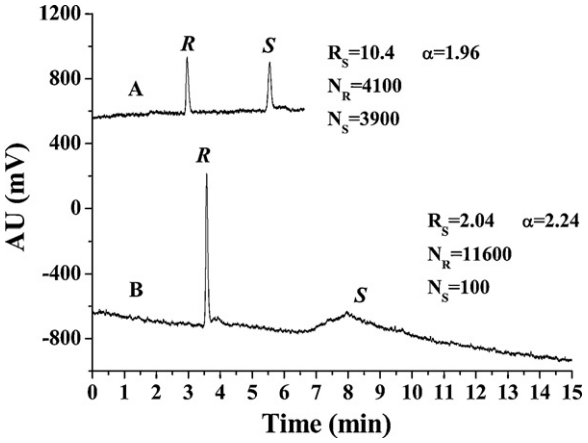

Fig. 3. The comparison figures of the separation of low (20%) (A) and high (80%) (B) cross-linked coating columns. Conditions: separation voltage, 12 kV; temperature, 25 °C; UV–vis detector, 238 nm; acetonitrile/10 mM acetate (pH 3.6) (80/20, v/v).

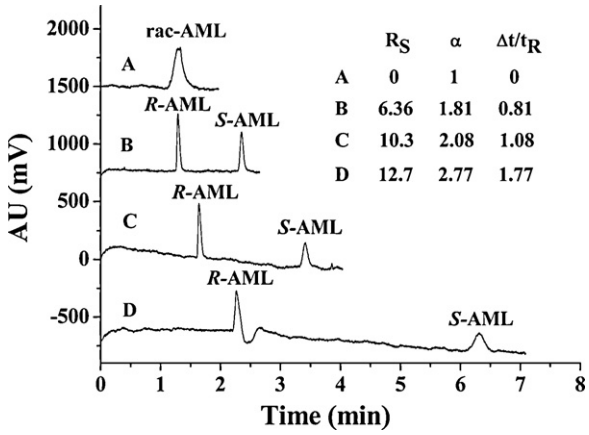

Fig. 4. Effects of the enantiomer separation of the different acetonitrile concentrations on (*S*)-amlodipine-imprinted coatings column. Sample: *rac*-amlodipine. Elution order: (*R*)-amlodipine followed by (*S*)-amlodipine. Conditions: separation voltage, 25 kV; temperature, 25 °C; UV–vis detector, 238 nm; acetonitrile/10 mM acetate (pH 3.6). (A) 90%, (B) 80%, (C) 70% and (D) 60%.

classical ratio in molecular imprinting, in the total monomers was synthesized. The CEC results of corresponding (*S*)-AML imprinted capillary were evaluated comparatively with regard to efficiencies, enantioselectivities and resolution of enantiomers (Fig. 3). It was observed that the liquid crystal MIP-coated capillary showed higher resolution (R_S = 10.4) than the liquid crystalline-free MIP coating (R_S = 2.04). Higher plate numbers of the template were also recorded for the liquid crystalline MIP capillary, which were about 39 times those of the liquid crystalline-free MIP with high level of EDMA. It should be noted that the characteristic band broadening for MIP-based separation was improved significantly on the liquid crystalline MIP capillary with low level of EDMA. In addition, the selectivity was superior in the liquid crystalline MIP capillary.

3.3. Effect of CEC parameters on separation of enantiomers

In this study, the pH effect in mobile phase (from 3.0 to 6.0) on separation of enantiomers was examined on the (*S*)-AML-imprinted coating with liquid crystalline (Table 2). A general increase in EOF with an increased pH was observed. The optimized eluent pH for separation was 3.6 in terms of the selectivity, normalized separation index and the resolution of the enantiomers, which can be explained by that the selectivity of MIP is maximal at a pH value nearing the pK_a value of the imprinted molecule [43].

The effect of ACN contents on enantiomer separation is shown in Fig. 4. When the ACN concentration was 60%, the EOF was too small and longer separation time was needed, although the highest normalized separation index was achieved. There was a trend that the separation factors and resolution for AML enantiomers decreased with the increase in the amount of ACN. When the ACN concentration was 90%, the separation of AML enantiomers disappeared. This result was in agreement with previous reports on MIP-coated capillaries for CEC enantiomer separation [36,40]. The optimized ACN volume was 80% in terms of resolution of the enantiomers and separation time.

The effect of salt concentration on the separation of enantiomers of *rac*-AML was investigated using different ionic strengths of electrolyte, from 5 to 20 mM HAc–NaAc (pH 3.6)/ACN (20:80, v/v) (Fig. 5). Both the retention time and the selectivity factor increased as the salt concentration in the electrolyte increased. However, higher salt concentration may result in peak broadening in spite of increased resolution. 10 mM was just selected since quite good separation performance was achieved within a proper analysis time, although somewhat better separation performance was obtained with a higher salt concentration at the expense of longer retention times.

Table 2
Enantiomer separations on *S*-AML-imprinted capillary at various electrolyte pH values.

pH	N_R (plate/m)	N_S (plate/m)	α	$\Delta t_R/t_{R1}$	R_s
3.0	7300	7790	2.05	1.05	7.13
3.6	13,300	12,900	1.96	0.96	10.4
4.2	14,500	12,200	1.54	0.54	5.86
5.0	15,500	13,800	1.51	0.51	5.25
6.0	15,900	15,800	1.34	0.34	3.33

CEC conditions: separation voltage, 12 kV; temperature, 25 °C; UV–vis detector, 238 nm; acetonitrile/10 mM acetate (80/20, v/v).

3.4. Van Deemter analysis

We also examined the influence of separation voltage on the EOF at the range of 3–25 kV using ACN/10 mM acetate (pH 3.6) (80/10, v/v) as the mobile phase. It was shown that with the increase of separation voltage, the EOF mobility had a linear increasing trend on the (*S*)-AML-imprinted capillary (data not shown). As depicted in Fig. 6, for the template, the relatively flat right portion of the *H*–*u* curves indicates an efficient mass-transfer process between

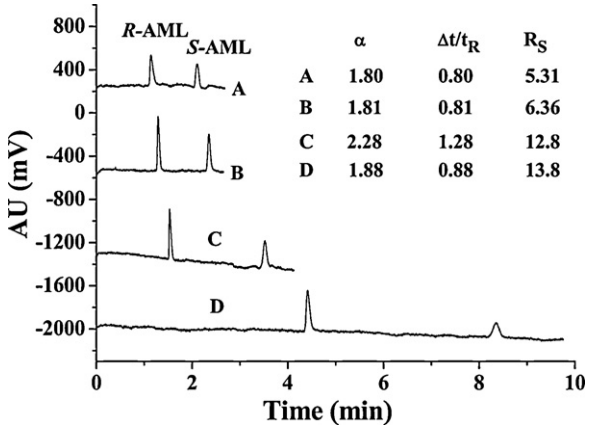

Fig. 5. Effects of the enantiomer separation of the different salt concentrations on the (*S*)-amlodipine-imprinted coatings column. Sample: *rac*-amlodipine. Elution order: (*R*)-amlodipine followed by (*S*)-amlodipine. Conditions: separation voltage, 25 kV; temperature, 25 °C; UV–vis detector, 238 nm; ACN/10 mM acetate (pH 3.6) (80/20, v/v). (A) 5 mM, (B) 10 mM, (C) 15 mM and (D) 20 mM.

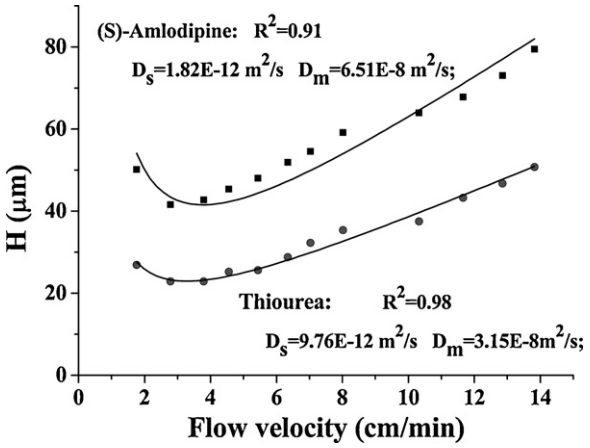

Fig. 6. Effect of voltage on the plate height (H) on (*S*)-amlodipine imprinted coating column with a porous polymer layer of 0.2 μm. The electrolyte used composed of acetonitrile/acetate (pH 3.6, 10 mM) (80/20, v/v). CEC experiments were performed by applying different voltages from 3 to 25 kV, respectively. (A) thiourea as EOF marker; (B) (*S*)-amlodipine.

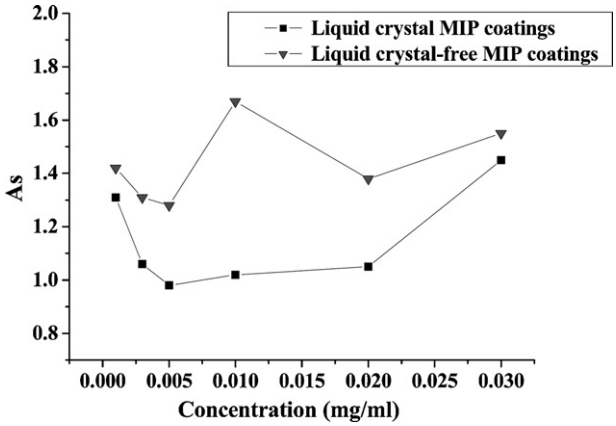

Fig. 7. Asymmetry factor (A_s) of *S*-AML versus sample load on the liquid crystal (A) and liquid crystal-free (B) MIP coatings.

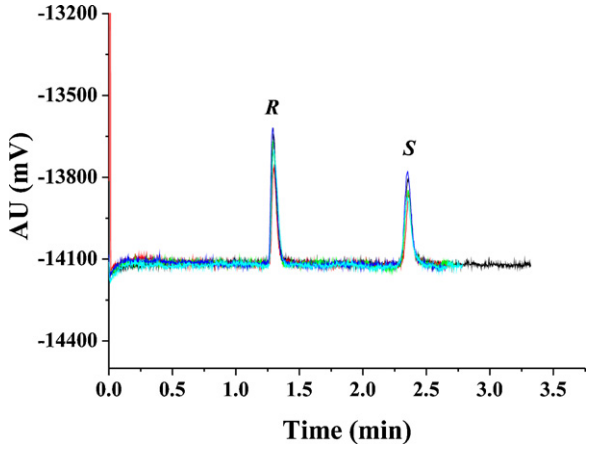

Fig. 8. Intra-column reproducibility of the enantiomer separation of amlodipine using (*S*)-amlodipine imprinted coating column. Sample: *rac*-amlodipine. Conditions: separation voltage, 25 kV; temperature, 25 °C; UV–vis detector, 238 nm; acetonitrile/10 mM acetate (pH 3.6) (80/20, v/v).

the mobile phase and the liquid crystal MIP coating. In other words, the resistance to mass transfer for the template can be negligible at the experimental conditions since the similar slopes of H–u curves was observed for unretained neutral thiourea, too. The result suggests that the MIP coating with liquid crystalline structure has some features in common with the improvements of the mass transfer and/or accessibility of the sites. Compared with previous result with a capillary of 25 μm-inner diameter [44], the trend of H–u data was different, which may be attributed to the difference in Joule heat due to the use of 100 μm-inner diameter in our work.

The Golay equation (Eq. (1)) enables a calculation of the theoretical performance of OT capillary columns [44]:

$$H = \frac{2D_m}{u} + \frac{d_c^2 u}{D_m} \cdot \frac{k^2}{16(1+k)^2} + \frac{d_f^2 u}{D_s} \cdot \frac{k}{(1+k)^2} \quad (1)$$

where d_c is the inner diameter of capillary, d_f is the thickness of the porous polymer layer, u is the linear flow velocity, D_s, an estimated diffusion coefficient in the stationary phase, and D_m is the diffusion coefficient in the mobile phase, which were calculated with the Wilke–Chang equation. The calculated curves fitted reasonably well with the experimental H–u data applying an estimated diffusion coefficient in the stationary phase $D_s = 1.82 \times 10^{-12}$ m^2/s. This value was almost 2 times lower than that of previous MIP coating with AML imprints [38], which suggests that the mass transfer and/or binding capacity were improved significantly on the liquid crystal MIP capillary.

3.5. Effect of sample loading on separation

The effect of sample loading on separation was studied by injecting different sample concentrations, ranging from 0.003 to 0.03 mg mL^{-1}. It was found that good separation efficiency and appropriate detection sensitivity were obtained. Compared with AML-imprinted coating with a thickness around 1–2 μm [43], less difference of column capacity was observed, suggesting that sample loading capacity of liquid crystal MIP coating was comparable to liquid crystal one. Furthermore, the peak shape, reflected in the peak asymmetry factor (A_s), is informative about the existence of non-linear binding isotherms and slow mass transfer of solute to the stationary phase [45]. It is possible to distinguish these effects by studying the dependence of A_s on sample load. Fig. 7 shows A_s as function of sample load on liquid crystal and liquid crystal-free imprinted coatings, respectively. As shown in Fig. 7, weak dependence of A_s on both sample load and flow-rate suggests the absence of slow adsorption/desorption on the liquid crystal MIPs reported here.

3.6. Reproducibility

Reproducibility of various CEC parameters is a critical consideration in the field of preparation and application of MIP coatings. The results of the retention time, column efficiency and resolution of (*R*)- and (*S*)-AML on the identical column and different batches of the low crosslinking MIP-coated capillary are shown in Fig. 8 and Table 3, respectively. The relative standard deviation (RSD) of inter-day reproducibility for the resolution of two enantiomers on a single capillary was lower than 1.5% (n = 5). However, RSD for the resolution from batch-to-batch preparation was 5% (n = 3). The results indicated that the liquid crystal low crosslinking MIP coat-

Table 3
Relative standard deviation (RSD) of reproducibility on liquid crystal-based capillaries with *S*-AML imprints.

	Inter-day		Batch-to-batch	
	R	*S*	*R*	*S*
Retention time (RSD%)	0.58	0.98	2.67	1.18
Column efficiency (RSD%)	1.16	0.65	2.33	3.20
Resolution (RSD%)	0.55		2.86	

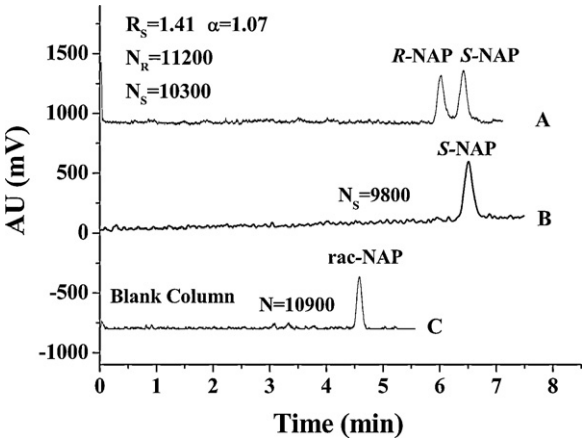

Fig. 9. Separation of *rac*-naproxen on (*S*)-naproxen-imprinted liquid crystal coating capillary containing low percentages of crosslinker. Conditions: separation voltage, 12 kV; temperature, 25 °C; UV–vis detector, 254 nm; acetonitrile/10 mM acetate (pH 3.6) (80/20, v/v).

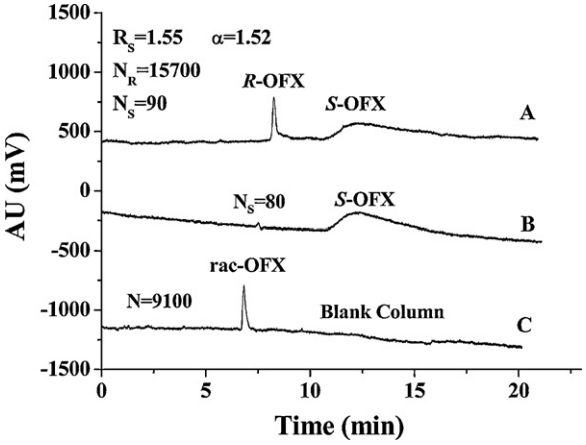

Fig. 10. Separation of enantiomers of *rac*-ofloxacine on (*S*)-ofloxacine-imprinted liquid crystal coating capillary containing low percentages of crosslinker. Conditions: separation voltage, 12 kV; temperature, 25 °C; UV–vis detector, 254 nm; acetonitrile/10 mM acetate (pH 5.0) (80/20, v/v).

ings had better reproducibility of preparation than that using a high level of crosslinker [38,40].

3.7. Separation of enantiomers of naproxen and ofloxacine with liquid crystal MIP at low crosslinking density

In order to prove the versatility of the low crosslinking liquid crystalline MIP columns, we also synthesized the MIP-coated capillaries using (*S*)-naproxen and (*S*)-ofloxacine as templates, respectively. Separation of enantiomers of naproxen and ofloxacine was achieved in their respective low crosslinking MIP columns (Figs. 9 and 10). The resolutions of *rac*-naproxen and *rac*-ofloxacine were 1.41 and 1.55, respectively. It should be noted that in the separation of *rac*-ofloxacine, a peak broadening of the template was observed. However, it was definitely separation of enantiomers on the MIP at low crosslinking density (20%), while imprinting does not work in general at such concentration of cross-linker.

4. Conclusion

We reported here for the first time a method of liquid crystal-based molecularly imprinted coating inside capillaries. Separation of enantiomers of racemic amlodipine, naproxen, and ofloxacin was achieved in CEC mode. Performance on the imprinted capillary coatings with low level of crosslinker was comparable to that recorded for CEC-based MIPs with high level of crosslinker [31,36]. In addition, the imprinted coating columns at low crosslinking level showed faster separation, higher column efficiency and more stable CEC results. The advantages of the low crosslinking MIP with liquid crystal are that good accessibility of binding sites and/or improved mass transfer can be obtained since a part of the chemical crosslinking is replaced by a physical one due to the interactions between the mesogens. Therefore, liquid crystal MIP coating grafted to rigid matrix will be expected to be used as stationary phase. We believe this proposed approach will open new perspectives toward highly selective and efficient MIPs stationary phase in the low crosslinking conditions.

Acknowledgments

This work was supported by the National Natural Science Foundation of China (Grant No. 21075090) and supported by the Hundreds Talents Program of the Chinese Academy of Sciences.

References

[1] G. Wulff, Angew. Chem. Int. Ed. 34 (1995) 1812.
[2] I.A. Nicholls, J. Mol. Recognit. 11 (1998) 79.
[3] G. Wulff, J. Liu, Acc. Chem. Res. 45 (2012) 239.
[4] C.A. Barrios, C. Zhenhe, F. Navarro-Villoslada, D. López-Romero, M.C. Moreno-Bondi, Biosens. Bioelectron. 26 (2011) 2801.
[5] F. Barahona, E. Turiel, A. Martín-Esteban, J. Chromatogr. A 1218 (2011) 7065.
[6] F. Puoci, G. Cirillo, M. Curcio, O.I. Parisi, F. Iemma, N. Picci, Expert Opin. Drug Deliv. 8 (2011) 1379.
[7] J. Haginaka, J. Sep. Sci. 32 (2009) 1548.
[8] G. Wulff, Chem. Rev. 102 (2002) 1.
[9] S.A. Piletsky, E.V. Piletskaya, T.L. Panasyuk, A.V. El'Skaya, R. Levi, I. Karube, G. Wulff, Macromolecules 31 (1998) 2137.
[10] R.M. Garcinuño, I. Chianella, A. Guerreiro, I. Mijangos, E.V. Piletska, M.J. Whitcombea, S.A. Piletsky, Soft Matter 5 (2009) 311.
[11] L.-N. Mu, X.-H. Wang, L. Zhao, Y.-P. Huang, Z.-S. Liu, J. Chromatogr. A 1218 (2011) 9236.
[12] J.-D. Marty, M. Tizra, M. Mauzac, I. Rico-Lattes, A. Lattes, Macromolecules 32 (1999) 8674.
[13] J.D. Marty, H. Gornitzka, M. Mauzac, Eur. Phys. J. E 17 (2005) 515.
[14] J.D. Marty, L. Labadie, M. Mauzac, C. Fournier, I. Rico-Lattes, A. Lattes, Mol. Cryst. Liq. Cryst. 411 (2004) 1603.
[15] C. Binet, D. Bourrier, M. Dilhan, D. Esteve, S. Ferrere, J.C. Garrigue, H. Granier, A. Lattes, A.M. Gue, M. Mauzac, A.F. Mingotaud, Talanta 69 (2006) 757.
[16] J.D. Marty, M. Mauzac, C. Fournier, Liq. Cryst. 29 (2002) 529.
[17] J.D. Marty, M. Mauzac, D. Lavabre, Mol. Cryst. Liq. Cryst. 437 (2005) 1307.
[18] M. Weyland, S. Ferrere, A. Lattes, A.-F. Mingotaud, M. Mauzac, Liq. Cryst. 35 (2008) 219.
[19] C. Binet, S. Ferrère, A. Lattes, E. Laurent, J.-D. Marty, M. Mauzac, A.-F. Mingotaud, G. Palaprat, M. Weyland, Anal. Chim. Acta 591 (2007) 1.
[20] F. Svec, Electrophoresis 30 (Suppl. 1) (2009) S68.
[21] J.-M. Lin, K. Uchiyama, T. Hobo, Chromatographia 47 (1998) 625.
[22] G. Chirica, V.T. Remcho, Electrophoresis 20 (1999) 50.
[23] M. Quaglia, E. De Lorenzi, C. Sulitzky, G. Caccialanza, B. Sellergren, Electrophoresis 24 (2003) 952.
[24] P. Spégel, L. Schweitz, S. Nilsson, Electrophoresis 22 (2001) 3833.
[25] P. Spégel, L. Schweitz, S. Nilsson, Anal. Chem. 75 (2003) 6608.
[26] F. Priego-Capote, L. Ye, S. Shakil, S.A. Shamsi, S. Nilsson, Anal. Chem. 80 (2008) 2881.
[27] X.-X. Shi, L. Xu, H.-Q. Duan, Y.-P. Huang, Z.-S. Liu, Electrophoresis 32 (2011) 1348.
[28] L. Schweitz, L.I. Andersson, S. Nilsson, Anal. Chem. 69 (1997) 1179.
[29] C. Cacho, L. Schweitz, E. Turiel, C. Perez-Conde, J. Chromatogr. A 1179 (2008) 216.
[30] M. Li, X. Lin, Z. Xie, J. Chromatogr. A 1216 (2009) 5320.
[31] H.F. Wang, Y.Z. Zhu, X.P. Yan, R.Y. Gao, J.Y. Zheng, Adv. Mater. 18 (2006) 3266.
[32] B.Y. Huang, Y.C. Chen, G.R. Wang, C.Y. Liu, J. Chromatogr. A 1218 (2011) 849.
[33] Z.S. Liu, Y.L. Xu, C. Yan, R.Y. Gao, J. Chromatogr. A 1087 (2005) 20.
[34] L. Schweitz, Anal. Chem. 74 (2002) 1192.
[35] Y.-C. Huang, C.-C. Lin, C.-Y. Liu, Electrophoresis 25 (2004) 554.
[36] S.A. Zaidi, W.J. Cheong, J. Chromatogr. A 1216 (2009) 2947.
[37] O. Brüggermann, R. Freitag, M.J. Whitcombe, E.N. Vulfson, J. Chromatogr. A 781 (1997) 43.

[38] Z.-H. Wei, X. Wu, B. Zhang, R. Li, Y.-P. Huang, Z.-S. Liu, J. Chromatogr. A 1218 (2011) 6498.
[39] J.Z. Tan, V.T. Remcho, Electrophoresis 19 (1998) 2055.
[40] X. Wu, Z.-H. Wei, Y.-P. Huang, Z.-S. Liu, Chromatographia 72 (2010) 101.
[41] S.A. Zaidi, W.J. Cheong, Electrophoresis 30 (2009) 1603.
[42] S.A. Zaidi, K.M. Han, D.G. Hwang, W.J. Cheong, Electrophoresis 31 (2010) 1019.
[43] B. Sellergren, K.J. Shea, J. Chromatogr. A 654 (1993) 17.
[44] S. Eeltink, F. Svec, J.M.J. Frécchet, Electrophoresis 27 (2006) 4249.
[45] J.C. Giddings, Anal. Chem. 35 (1963) 1999.